Preprints of the 21st IFAC World Congress (Virtual)
Berlin, Germany, July 12-17, 2020

Pilot Assessment of Fault-Tolerant PID Flight Controller for Elevator Efficiency Reduction via Hardware-In-the-Loop Simulations ⋆

Masayuki SATO * **Ryoichi TAKASE** ** **Shinji SUZUKI** ***

* *Aeronautical Technology Directorate, Japan Aerospace Exploration Agency, Mitaka, Tokyo 181-0015, Japan.*
(e-mail: sato.masayuki@jaxa.jp)
** *Department of Aeronautics and Astronautics, The University of Tokyo, Tokyo 113-8656, Japan.*
(e-mail: takase-aero@g.ecc.u-tokyo.ac.jp)
*** *Institute of Future Initiatives, The University of Tokyo, Tokyo 113-8656, Japan.*
(e-mail: tshinji@mail.ecc.u-tokyo.ac.jp)

Abstract: This note presents the pilot assessment of a Fault-Tolerant Control (FTC) law for elevator efficiency reduction via Hardware-In-the-Loop Simulations (HILS) with a research airplane MuPAL-α. The FTC is supposed to be a PID controller from the viewpoint of the practicality and applicability, *viz.*, conventional Stability/Control Augmentation System (S/CAS) structure is adopted. The PID-FTC is designed with the consideration of onboard actuator uncertainties as well as the possible loss of efficiency (from 0% loss up to 80% loss) in the framework of H_∞ control with `hinfstruct` command implemented in Matlab®. In HILS, the pilot is required to have steady climb and descent under the condition that the elevator efficiency is gradually reduced in a software level. HILS results indicate that the designed PID-FTC works well when the elevator efficiency decreases even under wind gust conditions.

Keywords: Fault-Tolerant Control (FTC), flight controller, Stability/Control Augmentation System (S/CAS), pilot assessment, Hardware-In-the-Loop Simulation (HILS).

1. INTRODUCTION

Fault-Tolerant Control (FTC) is one of the most important research topics in aeronautical community, because faults may directly lead to severe tragedic accidents with many casualties, such as Japan Airlines Flight 123 accident with over 500 casualties in 1985 (Anonymous, 1987, 2011), etc. On this issue, NASA has already developed Propulsion Controlled Aircraft (PCA), which controls aircraft motions using only thrust, and has demonstrated its applicability with F-15 and MD-11 (Tucker, 1999). The effort to improve maneuverability in faulty conditions is still on going. That is, several projects to improve Technology Readiness Level (TRL) of FTC and Fault Detection and Diagnosis (FDD) have been carried out in EU. For example, GARTEUR RECOVER (REconfigurable COntrol for Vehicle Emergency Return) (Edwards et al., 2010), EU-FP7 ADDSAFE (Advanced fault diagnosis for safer flight guidance and control) (Goupil and Marcos, 2014), and EU-FP7 RECONFIGURE (REconfiguration of CONtrol in Flight for Integral Global Upset REcovery) (Goupil et al., 2015) have been conducted to improve TRL in FTC and FDD. Similarly to the situations in EU, Japanese aeronautical community has also developed FTC technologies. For example, FTC design using neural network (Suzuki and Yanagida, 2008) and its flight demonstration (Masui et al., 2008) using a research airplane MuPAL-α (shown in Fig. 1), etc. have been conducted.

Fig. 1. Research airplane MuPAL-α

The effort to increase TRL in FTC is still necessary, and thus a collaborative research project named "Validation of Integrated Safety-enhanced Intelligent flight cONtrol (VISION)" between EU and Japan was conducted as one of the research projects of Horizon2020 from February 2016 to August 2019. This project had two objec-

⋆ This work was supported by the EU Horizon 2020 research and innovation programme (GA N. 690811) and the Japan New Energy and Development Organization (GA N. 062800), as a part of the EU/Japan research project VISION.

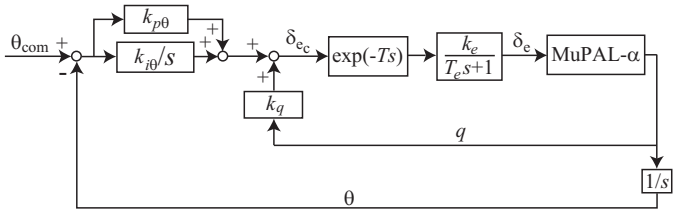

Fig. 2. Block diagram of S/CAS for longitudinal motion of MuPAL-α

tives, i.e. the development of visually supported navigation system using an Unmanned Aerial Vehicle (UAV) when GPS signals are not normal, and the applicability assessment of FTC and FDD using MuPAL-α (Masui and Tsukano, 2000). The former topic results have been reported in (Watanabe et al., 2019), etc., and this paper focuses on the latter topic. In particular, this note aims to report the pilot assessment of PID-based FTC, in short PID-FTC, with Hardware-In-the-Loop Simulations (HILS) of MuPAL-α. The pilot assessment of flight controllers is a necessary step to implement them to practical systems, which is the main motivation of this research note.

The remainder is organized as follows: Section 2 summarizes the design of a PID-FTC which is robust against the uncertainties related to the onboard elevator actuator as well as the efficiency reduction of elevator; Section 3 presents the pilot assessment of the designed PID-FTC via HILS with artificial reductions of elevator efficiency; Section 4 gives concluding remarks.

2. PID-FTC DESIGN

Although the design procedure has already been reported in Takase et al. (2019), the controller has been updated since then, thus the detailed description on PID-FTC design is given below.

The block diagram of Stability/Control Augmentation System (S/CAS) is depicted in Fig. 2, where k_q denotes the pitch rate (q in Fig. 2) feedback gain in SAS, $k_{p\theta}$ and $k_{i\theta}$ denote the Proportional-Integral (PI) gains for pitch angle error ($\theta_{com} - \theta$ in Fig. 2) in CAS, θ_{com} denotes the pitch angle command given by pilot, θ denotes the pitch angle, δ_{e_c} denotes the elevator angle deflection command, and δ_e denotes the elevator angle deflection. The state-space representation of the linearized longitudinal motions of MuPAL-α at a TAS (True Air Speed) of 77.5 [m/s] and an altitude of 1524 [m] is shown in the appendix. The linearized motions of MuPAL-α have good fidelity to the actual nonlinear motions as demonstrated in (Sato and Satoh, 2011); however, the onboard actuator system has relatively large uncertainties. To represent the uncertainties, in (Sato and Satoh, 2011), uncertain bounded delays, which is given as $\exp(-Ts)$ in Fig. 2, were introduced, and the controllers which are designed to be robust against the uncertain bounded delays represented with Linear Fractional Transformation (LFT) representation worked very well. In this note, another approach (i.e. weighting function approach to compensate for the maximum delay), which has been widely recognized (Skogestad and Postlethwaite, 2005) and has also been used in (Sato, 2018) for the lateral-directional motion control of MuPAL-α, is adopted.

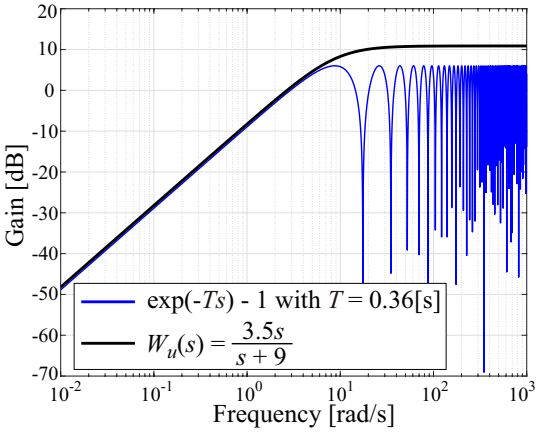

Fig. 3. Gain plots of weighting function $W_u(s)$ for actuator uncertainty given as $\exp(-Ts) - 1$

In this note, the efficiency reduction of elevator should be also incorporated. To this end, the efficiency factor f is introduced in the actuator model. That is, the actuator dynamics including uncertain delays and efficiency reduction are modeled as follows:

$$\delta_e = f \frac{k_e}{T_e s + 1} \exp(-Ts)\delta_{e_c} \tag{1}$$

where $f \in [0.2, 1.0]$ denotes the elevator efficiency, $k_e = 0.86$ denotes the actuator gain, $T_e = 0.03$ denotes the time constant of the first-order actuator model, and T [s] $\in [0.06, 0.36]$ denotes the uncertain delay which captures the uncertainties related to the onboard elevator actuator.

Note that (1) is represented as $f\frac{k_e}{T_e s+1}[1 + (\exp(-Ts) - 1)]$, the nominal actuator is then set as $\delta_e = \frac{k_e}{T_e s+1}\delta_{e_c}$ and the perturbation "$\exp(-Ts) - 1$" is introduced for the consideration of the uncertainties. Furthermore, similarly to (Sato, 2018), the following weighting function is introduced to cover the magnitude of the supposed perturbation, i.e. $\exp(-Ts) - 1$ with $T = 0.36$.

$$W_u(s) = \frac{3.5s}{s + 9} \tag{2}$$

The gain plots of $W_u(s)$ in (2) and $\exp(-Ts) - 1$ with $T = 0.36$ [s] are shown in Fig. 3, which confirms that the gain of the weighting function $W_u(s)$ in (2) covers the gain of the supposed perturbation $\exp(-0.36s) - 1$.

The requirement for S/CAS is to have good tracking for pitch angle control. A weighting function W_e for $\theta_{com} - \theta$ is thus introduced to impose this requirement. After several trial-and-errors, the following W_e is set.

$$W_e(s) = \frac{33.69s + 15}{165s + 1} \tag{3}$$

The choice of this weighting function is based on the rule that the large gain in the low frequencies leads to good tracking performance for low frequency command and that the large cross-over frequency increases the frequency of trackable command.

The PID-FTC is designed in the framework of H_∞ control; however, there exist two scalar uncertainties, i.e. the fictitious uncertainty block Δ_e for tracking performance and the uncertainty block Δ_u for actuator uncertainty. That is, the problem is not a pure H_∞ problem. Then, a constant scaling matrix L which is compatible to $\mathsf{diag}(\Delta_e, \Delta_u)$ is

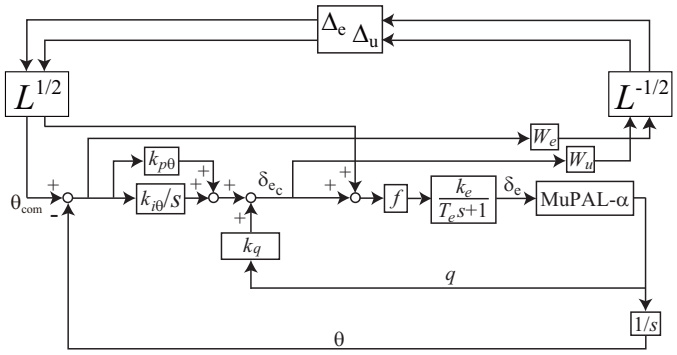

Fig. 4. Block diagram for designing PID-FTC via scaled H_∞ control

introduced, *viz.*, $L = \mathsf{diag}\,(l_1, l_2)$ with positive scalars l_1 and l_2 is introduced to reduce conservatism due to multiple uncertainty blocks. In the end, the block diagram for designing PID-FTC becomes the one in Fig. 4.

In the controller design, the efficiency reduction has already been incorporated using "f" as in Fig. 4, and the generalized plant then becomes parameter-dependent with respect to f; however, `hinfstruct` command cannot directly handle parameter-dependent plant systems. To tackle this issue, "multiple model approach" (Ackermann, 1985) is used; that is, five plant models with $f = \{0.2, 0.4, 0.6, 0.8, 1.0\}$ is set, and a single common S/CAS gains and a single common scaling matrix L for the five models are designed. By following the method above, a PID-FTC, i.e. S/CAS which is robust against the uncertainties related to the onboard elevator actuator as well as the efficiency reduction of elevator, will be designed.

With six random initial gains for `hinfstruct` command, the following PID-FTC gains are obtained achieving 0.995 of the maximum optimal scaled H_∞ norm for the five plant models with $L^{1/2} = \mathsf{diag}(8.081, 45.987)$.

$$k_q = 0.447,\ k_{p\theta} = -1.570,\ k_{i\theta} = -2.125 \qquad (4)$$

Fig. 5 shows the gain plots from θ_{com} to $\theta_{com} - \theta$ for the supposed elevator efficiency reduction models with $\Delta_u = \pm 1$. This figure confirms that the obtained PID-FTC gains have an ability to track pitch angle command with its frequency in $[0, 0.3]$ [rad/s] under the supposed elevator efficiency reduction as well as the supposed delays $\exp(-Ts)$ with $T = 0.36$ [s]. Note that the closed-loop system with $\Delta_u = 1$ corresponds to the controlled MuPAL-α with the maximum supposed delay for T, i.e. $T = 0.36$.

Fig. 6 shows the linear simulation results to confirm control performance of the designed PID-FTC. Although control performance for the minimum supposed efficiency (20 %) is not so good, it is confirmed that the designed PID-FTC tries to track the given pitch angle command even under significantly reduced elevator efficiency.

3. PILOT ASSESSMENT OF PID-FTC

As it is confirmed that the designed PID-FTC has an ability to track pitch angle command under possible elevator efficiency reduction with linear simulations in Fig. 6, pilot assessment for the designed PID-FTC with HILS, in which

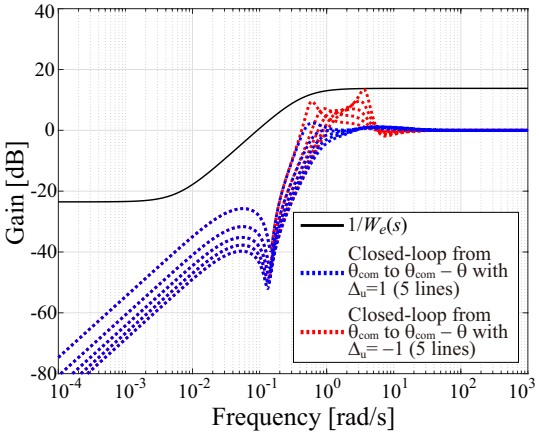

Fig. 5. Gain plots from θ_{com} to $\theta_{com} - \theta$ for ten plant models with $f = \{0.2, 0.4, 0.6, 0.8, 1.0\}$ and $\Delta_u = \pm 1$

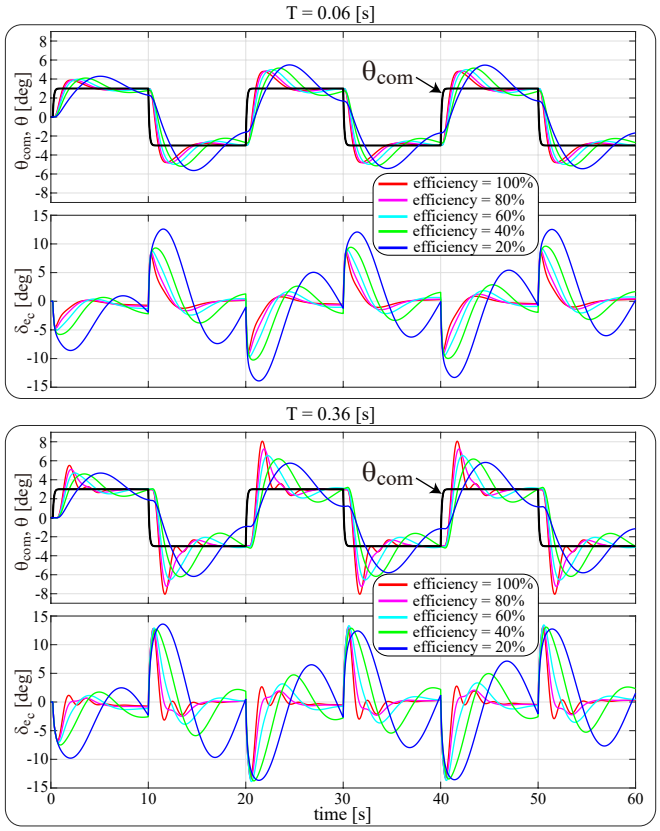

Fig. 6. Linear simulations for various elevator efficiency

nonlinear equations with aerodynamic coefficient maps are used, is conducted. The fidelity of the nonlinear equations with aerodynamic coefficient maps has been confirmed and demonstrated in Sato and Satoh (2011).

The main objective of HILS is to get pilot assessment for the designed PID-FTC, and thus practical pilot request is mandatory to obtain an appropriate pilot assessment. Thus, the pilot is requested to have steady climb with Rate-Of-Climb (ROC)=500[fpm](= 2.62[m/s]) or steady descent with ROC=−500[fpm](= −2.62[m/s]). However, the elevator efficiency degrades during the simulations without notifying the pilot. Thus, if the pilot does not realize the deterioration of maneuverability, then it can

be concluded that the PID-FTC has good control performance as an FTC.

In general, it is recommended to have tests with several (not so many, but more than single) pilots. Though, as a primitive test, we conducted HILS with a single pilot who has flight experience over 5500 hours as pilot-in-command with several types of aircraft including Cessna, Beechcraft, Aero Commander, etc.

In the figures showing HILS results, wind gust (u_g in the forward-backward direction and w_g in the upward-downward direction) is denoted by dotted red lines, and commands (pitch angle command given by the pilot and elevator angle deflection command given by the PID-FTC) are denoted by dotted blue lines. Other variables related to MuPAL-α's motions are given by solid black lines, *viz.*, u_a denotes the forward-backward air velocity deviation, w_a denotes the upward-downward air velocity deviation, θ denotes the pitch angle deflection, and δ_e denotes the elevator angle deflection. For reference, engine torque deviation, TAS deviation and the realized ROC are also given by solid black lines.

Before the pilot assessment for PID-FTC under reduced elevator efficiency, the control performance with fault-free elevator is examined. The result is shown in Fig. 7, which confirms that the designed PID-FTC faithfully tracks the pitch angle command given by pilot.

Then, pilot assessment under faulty elevator is conducted. Firstly, HILS tests without wind gust are conducted. One example is shown in Fig 8, where almost steady climb with ROC= 500[fpm] was kept with a slight TAS increase and almost the steady pitch angle until elevator efficiency reduced to 50 $\sim$ 40%. However, after the efficiency dropped to 30%, then the oscillations of ROC values became large and it can be concluded that keeping steady climb was hard. The pilot comment is as follows.

- During the flight, he didn't realize the maneuverability deterioration; however, when he tried to control the aircraft with zero ROC after climbing, he felt slightly sluggish in maneuverability, and slight oscillations of ROC values were observed. However, he felt no changes for maneuverability in climb phase.

Next, HILS tests under gusty conditions are conducted. Two examples are shown in Fig. 9 (climb) and Fig. 10 (descent). In both cases, although TAS was almost steadily kept, it can be found that the steady climb or descent was not so easy due to wind gust even when the efficiency was not so severely reduced. However, as is obvious, the difficulty became much hard after the efficiency reduced to less than 50%. The pilot comment is as follows.

- During these flights, it was indeed not so easy to maintain the steady rate for climb or descent. However, due to the lack of acceleration, he couldn't identify the cause of the oscillatory motions; that is, he couldn't determine the oscillatory motions were caused by wind gust or the deterioration of maneuverability. In this sense, he couldn't identify the maneuverability deterioration under windy condition.

In summary, in HILS, pilot didn't clearly recognize the maneuverability deterioration, i.e. loss of elevator efficiency.

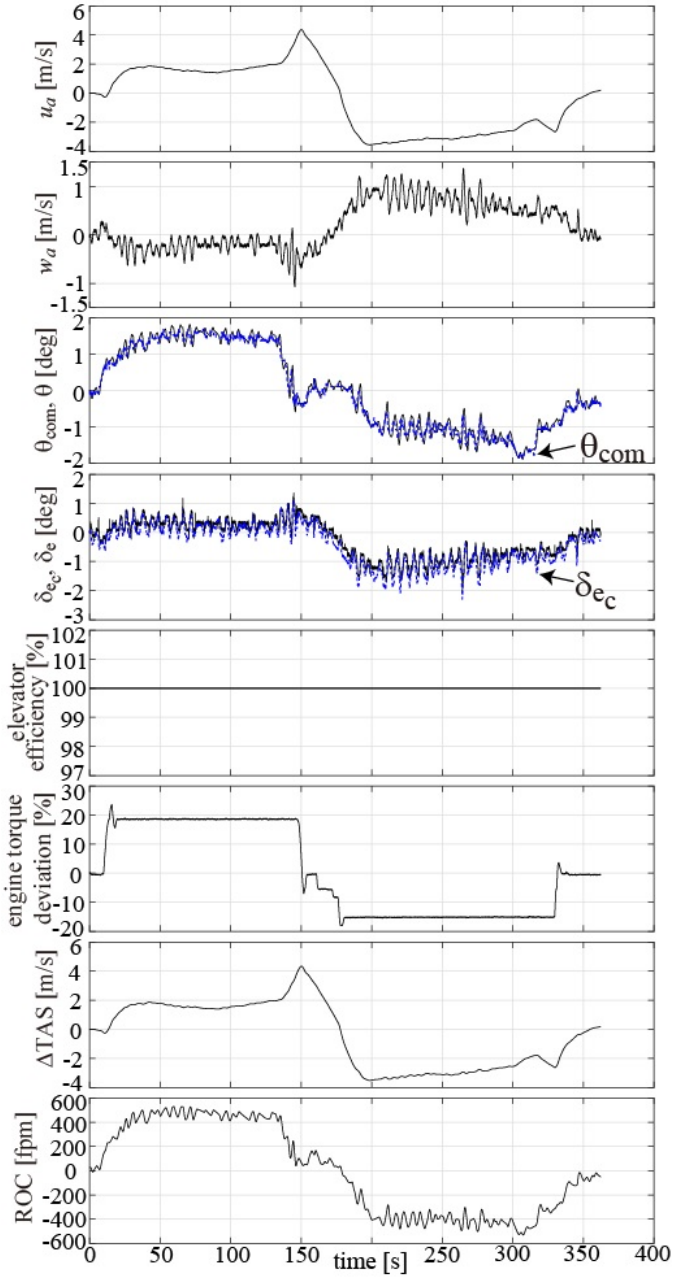

Fig. 7. HILS result without wind gust under fault-free elevator efficiency (climb and descent) (Initial TAS = 75.0 [m/s])

He felt sluggish maneuverability in calm condition; however, it was hard to identify the cause in windy condition due to the lack of acceleration. This indicates that the designed PID-FTC has no apparent problem in maneuverability under reduced elevator efficiency; however, flight tests may be necessary for rigorous pilot assessment of the designed PID-FTC.

4. CONCLUSIONS

This note presents the pilot assessment of the longitudinal Proportional-Integral-Derivative (PID)-based Fault-Tolerant Control (FTC) law, which is robust against the uncertainties related to the onboard actuator as well as the elevator efficiency reduction, for a research airplane

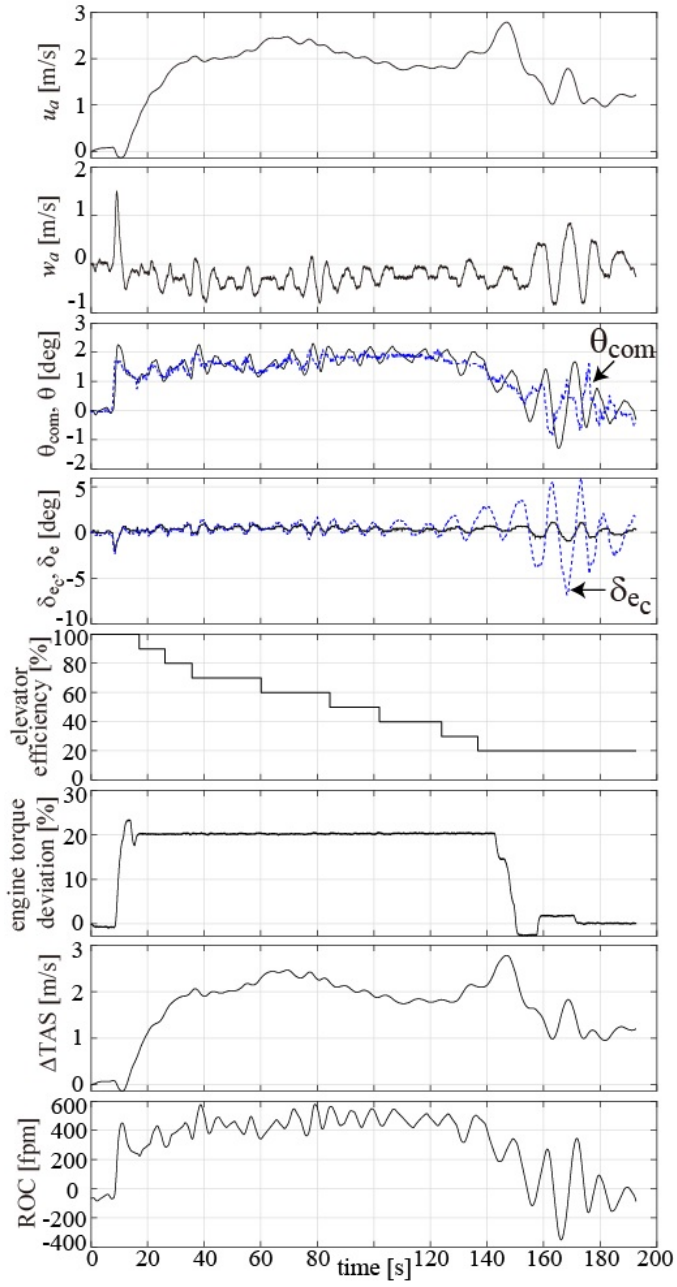

Fig. 8. HILS result without wind gust (climb) (Initial TAS = 76.3 [m/s])

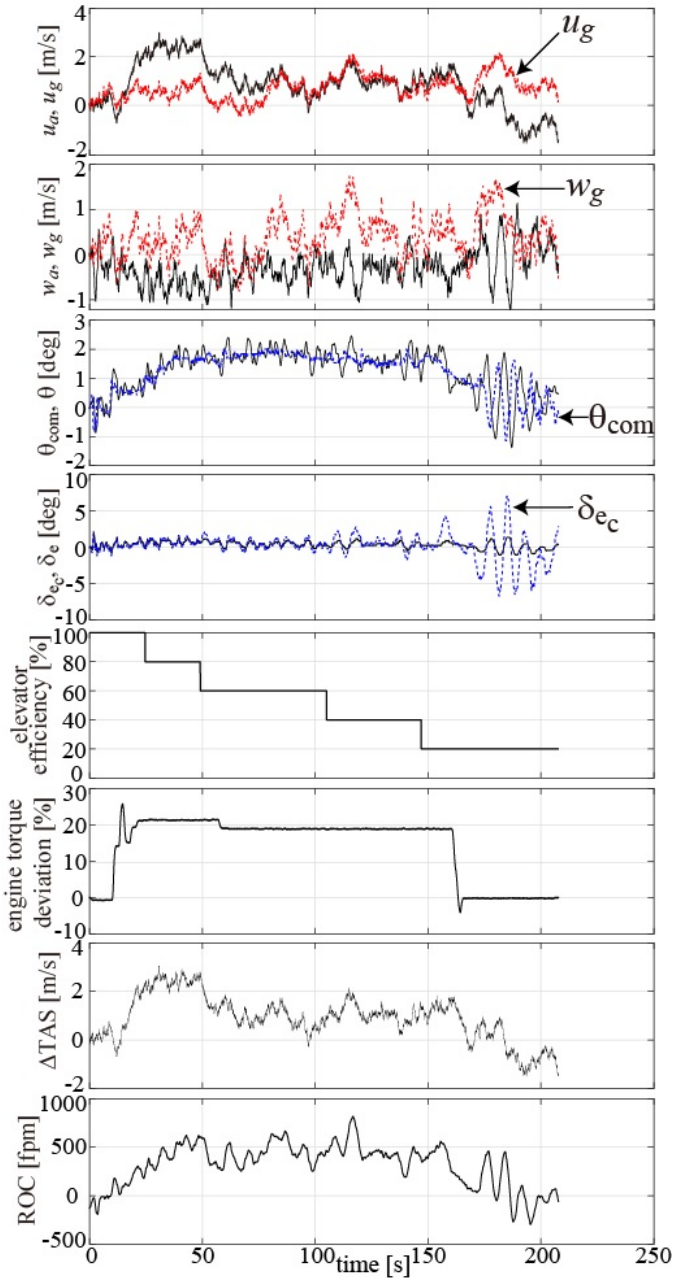

Fig. 9. HILS result with wind gust (climb) (Initial TAS = 75.7 [m/s])

MuPAL-α. The PID-FTC is designed using `hinfstruct` command implemented in Matlab® for multiple models representing the elevator efficiency reductions. After checking control performance with linear simulations, Hardware-In-the-Loop Simulations (HILS) are conducted to obtain pilot assessment. The HILS results indicate that the designed PID-FTC has no serious problem for maneuverability even under reduced elevator efficiency; however, flight tests may be necessary for rigorous pilot assessment, because HILS have neither physical motion nor acceleration.

ACKNOWLEDGEMENTS

The authors give sincere acknowledgements to Mr. Morokuma and Mr. Hosoya for their support in HILS.

REFERENCES

Ackermann, J. (1985). *Uncertainty and Control*, volume 70 of *Lecture Notes in Control and Information Sciences*, chapter Chapter 4: Multi-Model Approaches to Robust Control System Design, 108–130. Springer-Verlag, Berlin Heidelberg. doi:10.1007/BFb0007278.

Anonymous (1987). Aircraft accident investigation report on Boeing 747SR-100, JA8119. Technical Report 2, Japan Transport Safety Board. URL `http://www.mlit.go.jp/jtsb/aircraft/rep-acci/62-2-JA8119.pdf`. (in Japanese).

Anonymous (2011). Commentary on aircraft accident investigation report on Boeing 747SR-100, JA8119. Technical report, Japan Transport Safety Board. URL `http://www.mlit.go.jp/jtsb/kaisetsu/`

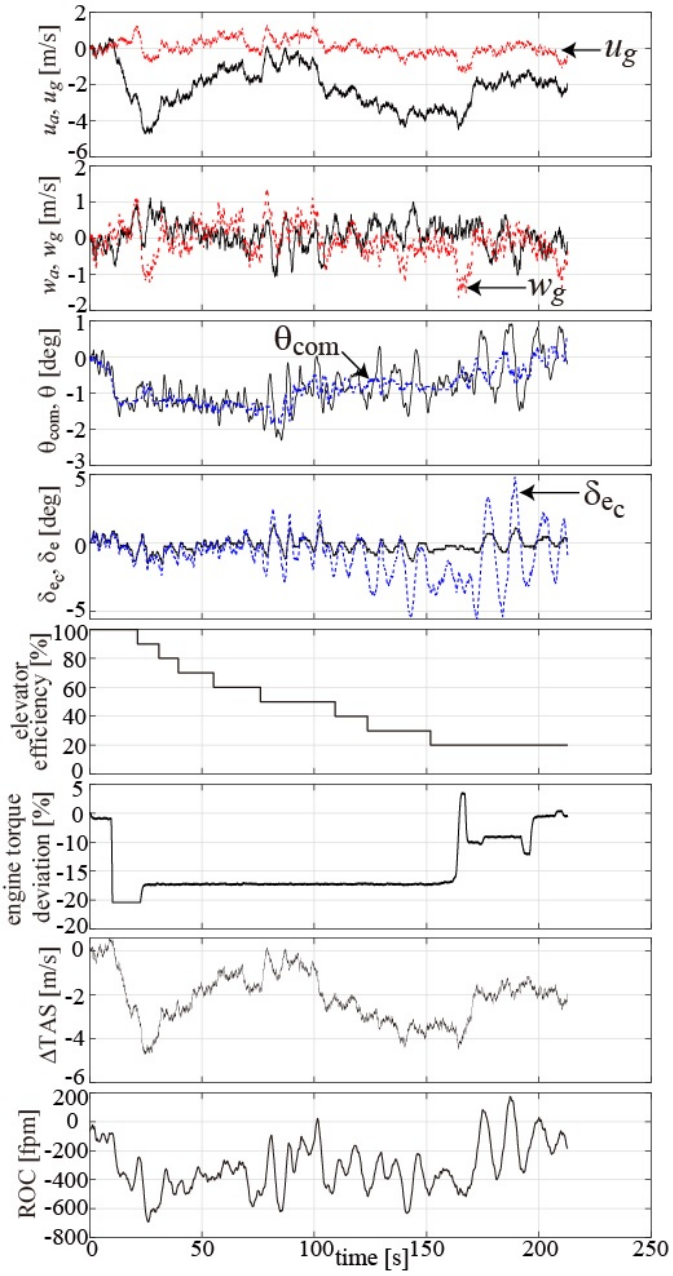

Fig. 10. HILS result with wind gust (descent) (Initial TAS = 76.5 [m/s])

nikkou123-kaisetsu.pdf. (in Japanese).

Edwards, C., Lombaerts, T., and Smaili, H. (2010). *Fault Tolerant Flight Control: A Benchmark Challenge*. Springer.

Goupil, P., B.-Bauxell, J., Marcos, A., Rosa, P., Kerr, M., and Dalbies, L. (2015). An overview of the FP7 RECONFIGURE project: Industrial, Scientific and Technological Objectives. In *9th IFAC Symposium on Fault Detection, Supervision and Safety for Technical Processes SAFEPROCESS 2015*, 976–981. IFAC, Paris, France.

Goupil, P. and Marcos, A. (2014). The European ADDSAFE project: Industrial and academic efforts towards advanced fault diagnosis. *Control Engineering Practice*, 31, 109–125.

Masui, K., Tomita, H., and Yanagida, A. (2008). Research and development for fault tolerant flight control system - part 2 flight experiments. In *26th Congress of the International Council of the Aeronautical Sciences*. ICAS 2008-5.10.2.

Masui, K. and Tsukano, Y. (2000). Development of a new in-flight simulator MuPAL-α. In *AIAA Modeling and Simulation Technologies Conference*. AIAA, Denver, CO. doi:10.2514/6.2000-4574. AIAA 2000-4574.

Sato, M. (2018). Gain-scheduled flight controller using bounded inexact scheduling parameters. *IEEE Transactions on Control Systems Technology*, 26(3), 1074–1082. doi:10.1109/TCST.2017.2692750.

Sato, M. and Satoh, A. (2011). Flight control experiment of multipurpose-aviation-laboratory-α in-flight simulator. *Journal of Guidance, Control, and Dynamics*, 34(4), 1081–1096. doi:10.2514/1.52400.

Skogestad, S. and Postlethwaite, I. (2005). *Multivariable Feedback Control*. John Wiley & Sons, Inc., West Sussex, England. Second edition.

Suzuki, S. and Yanagida, A. (2008). Research and development for fault tolerant flight control system - part 1 intelligent flight control system. In *26th Congress of the International Council of the Aeronautical Sciences*. ICAS 2008-5.10.1.

Takase, R., Suzuki, S., and Sato, M. (2019). Design of a fault-tolerant PID flight controller with structured H_∞ synthesis. In *Proceedings of the 50th JSASS Annual Meeting*. JSASS, Tokyo, Japan. (in Japanese).

Tucker, T. (1999). Touchdown: The Development of Propulsion Controlled Aircraft at NASA Dryden. Technical report, NASA. URL `https://ntrs.nasa.gov/archive/nasa/casi.ntrs.nasa.gov/20000025333.pdf`.

Watanabe, Y., Manecy, A., Hiba, A., Nagai, S., and Aoki, S. (2019). Vision-integrated navigation system for aircraft final approach in case of GNSS/SBAS or ILS failures. In *AIAA GNC conference, SciTech Forum*. AIAA, San Diego, USA. doi:10.2514/6.2019-0113.

Appendix A. STATE-SPACE MODEL

The state-space representation of the linearized longitudinal motions of MuPAL-α at a TAS (True Air Speed) of 77.5 [m/s] and an altitude of 1524 [m] is given as follows:

$$\begin{cases} \dot{x}_p = A_p x_p + B_p u_p \\ y_p = C_p x_p + D_p u_p \end{cases},$$

where $x_p = [u[\mathrm{m/s}]\ w[\mathrm{m/s}]\ q[\mathrm{rad/s}]\ \theta[\mathrm{rad}]]^T$ denotes the state, $u_p = \delta_e[\mathrm{rad}]$ denotes the control input, and $y_p = [q\ \theta]^T$ denotes the measurement output. Here, u and w respectively denote the forward-backward and upward-downward airspeed, q denotes the pitch rate, θ denotes the pitch angle, and δ_e denotes the elevator angle.

The state-space matrices $\left[\begin{array}{c|c} A_p & B_p \\ \hline C_p & D_p \end{array}\right]$ are given as follows:

$$\left[\begin{array}{cccc|c} -0.0189 & 0.1481 & -3.5908 & -9.7956 & 0.3050 \\ -0.1885 & -1.2670 & 75.4565 & -0.4663 & -6.4099 \\ 0.0047 & -0.0647 & -2.2180 & 0 & -5.2350 \\ 0 & 0 & 1 & 0 & 0 \\ \hline 0 & 0 & 1 & 0 & 0 \\ 0 & 0 & 0 & 1 & 0 \end{array}\right].$$